Spatiotemporal Drought Analysis at Country Scale Through the Application of the STAND Toolbox

Diaz, Vitali; Corzo, Gerald A.; Van Lanen, Henny A.J.; Solomatine, D.P.

Citation (APA)
Diaz, V., Corzo, G. A., Van Lanen, H. A. J., & Solomatine, D. P. (2019). Spatiotemporal Drought Analysis at Country Scale Through the Application of the STAND Toolbox. In G. Corzo, & E. A. Varouchakis (Eds.), *Spatiotemporal Analysis of Extreme Hydrological Events* (pp. 77-93). Elsevier. https://doi.org/10.1016/B978-0-12-811689-0.00004-5

Important note
To cite this publication, please use the final published version (if applicable).
Please check the document version above.

4

Spatiotemporal Drought Analysis at Country Scale Through the Application of the STAND Toolbox

Vitali Diaz[1,2], Gerald Corzo[1], Henny A.J. Van Lanen[3], Dimitri P. Solomatine[1,2]

[1]UNESCO-IHE INSTITUTE FOR WATER EDUCATION, DELFT, THE NETHERLANDS; [2]WATER RESOURCES SECTION, DELFT UNIVERSITY OF TECHNOLOGY, DELFT, THE NETHERLANDS; [3]HYDROLOGY AND QUANTITATIVE WATER MANAGEMENT GROUP, WAGENINGEN UNIVERSITY, WAGENINGEN, THE NETHERLANDS

1. Introduction

Drought is a natural phenomenon whose impacts generate many economic and human losses (Below et al., 2007; Sheffield and Wood, 2011; Tallaksen and Van Lanen, 2004). Different definitions of drought have been proposed, according to the discipline from where drought is addressed (Bachmair et al., 2016; Mishra and Singh, 2010). The general consensus is that it is an anomaly originating in precipitation and temperature, whose further effects are observed in other components of the hydrological cycle such as soil moisture and runoff, affecting human activities (Tallaksen and Van Lanen, 2004; Van Loon, 2015). However, the spatial extent and duration of drought are not explicitly contemplated in such definitions. Many studies of global models that explore drought require arbitrary steps to define the size (threshold) that can be used to consider an event as extreme or even normal. In this sense, one drought event in a large region can be generalized in a particular time, even if the region does not show drought in its entire area but only in a small part.

To estimate drought magnitude and duration, drought indicators or indices (DIs) are often used. A DI is a mathematical formulation that quantifies the water anomaly in a hydrometeorological variable (Mishra and Singh, 2010, 2011). When the DI is computed over a region in a spatial way, the spatial extent of drought is estimated by performing a spatiotemporal method (e.g., Corzo Perez et al., 2011; Hannaford et al., 2011; Herrera-Estrada et al., 2017; Hisdal and Tallaksen, 2003; Lloyd-Hughes, 2012; Peters et al., 2006; Sheffield et al., 2009; Tallaksen et al., 2009; Tallaksen and Stahl, 2014; Van Huijgevoort et al., 2013; Vicente-Serrano, 2006; Zaidman et al., 2002). Currently, monitoring of drought

magnitude, duration, and area over a region is carried out through drought-monitoring systems. These systems are fed with hydrometeorological variables. The outcomes generated are known as drought-monitoring products. Drought indicator databases are part of this information. These drought-related data perform more detailed analyses on the spatiotemporal development of drought.

It has been highlighted that a better analysis of drought allows the development and implementation of more successful national policies for the mitigation of drought impacts (World Meteorological Organization (WMO), 2006). The WMO also points out that for the reduction of negative drought impacts it is necessary to develop technologies and methods to improve the characterization of drought.

The objective of this chapter is to introduce the Spatio-Temporal ANalysis of Drought (STAND) toolbox. The tool includes two methodologies for the spatiotemporal characterization of drought: (1) Non-Contiguous Drought Area (NCDA) analysis (Corzo Perez et al., 2011), and (2) Drought DuRation, SeveriTy, and Intensity Computing (DDRASTIC). The use of STAND is illustrated with two case studies: Mexico and India. After this introductory section, the NCDA and DDRASTIC methodologies are described, as well as the STAND components. Then, case studies and data are presented. Following this, the results and discussion section is shown.

2. Spatio-Temporal ANalysis of Drought Toolbox

2.1 STAND Analysis

The analysis of drought proposed here can be performed in four main steps aiming at the description of how drought evolves in space (drought area), and how this spatial area changes over time. As mentioned, drought is defined here as an anomaly in the hydrometeorological variable under analysis. This anomaly is detected with the help of a DI. Three types of drought events are defined here based on the way data are processed: time series, spatial, and spatiotemporal events.

Step 1. Temporal analysis: calculation of the region-aggregated drought indicator, as well as computation of the time series events and their duration and deficit.

Step 2. Spatiotemporal analysis: integration of the time series events into aggregated areas of drought, and calculation of the percentage of drought area (PDA) in each time step.

Step 3. Characterization of the spatiotemporal events.

Step 4. Visualization and analysis of results.

2.2 Temporal Analysis (Step 1)

Fig. 4.1 shows a time series of a DI whose values oscillate from −3 to 3. The negative values are associated with the drought anomalies. In grid data, each cell has a DI time series, and over each one the characterization of time series events indicated in this step
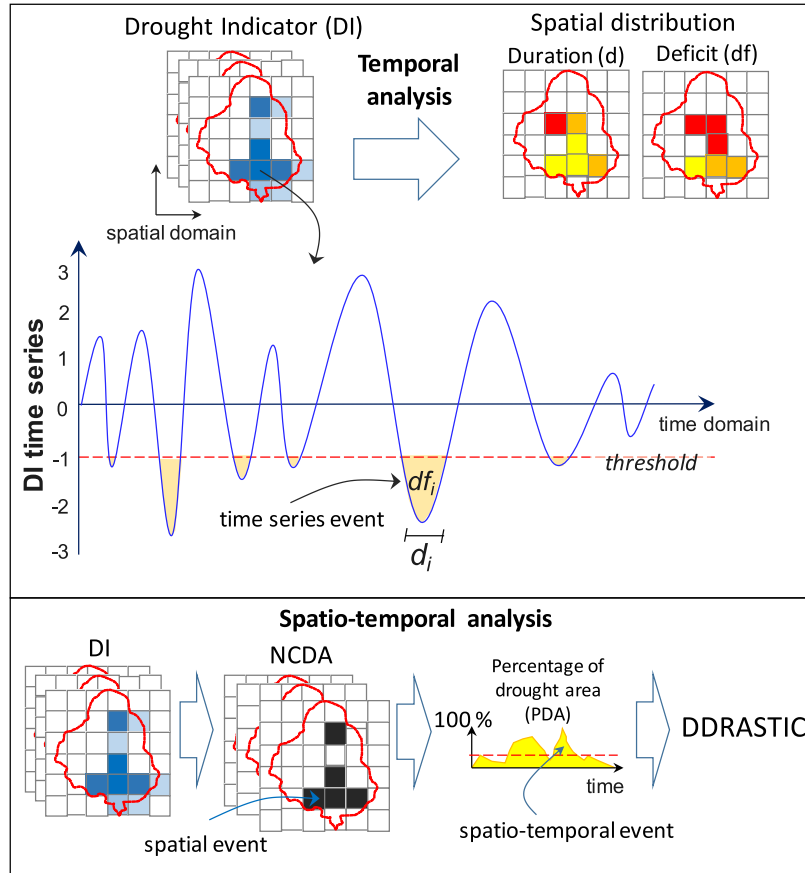
FIGURE 4.1 Schematic overview of the methodologies for drought analysis in the Spatio-Temporal ANalysis of Drought (STAND) toolbox: Non-Contiguous Drought Area (NCDA) analysis and Drought DuRAtion, SeveriTy, and Intensity Computing (DDRASTIC).

is carried out. Following Mckee et al. (1993), a time series event starts at time *ts* when the DI value is below a set threshold (T) and ends at time *te* when DI is above the threshold. Duration (d) and deficit (df) of each ith time series event are computed with Eqs. (4.1) and (4.2), respectively.

$$d_i = te - ts \tag{4.1}$$

$$df_i = \sum_{t=ts}^{te}(DI(t) - T). \tag{4.2}$$

The deficit is standardized and expressed as a percentage with Eq. (4.3):

$$dfs_i = 100 \times df_i / \overline{x} \tag{4.3}$$

where dfs_i is the standardized deficit of the ith time series event and $\bar{x}$ is the mean of the deficit values of the analyzed time series.

To summarize d and df computed over each time series, their median values are calculated in each cell. In this way, maps of the spatial distribution of d and df are obtained.

2.3   Spatiotemporal Analysis (Step 2)

This procedure follows Corzo Perez et al. (2011). To be able to take into account how much the spatial coverage of drought is changing, we need to estimate the amount of area affected in each time step. Therefore the DI values have to be converted into events (binary representation) based on a feasible threshold. The threshold method is well known and its algorithm is described in Eq. (4.4). At each time step (t), ones and zeros are used to indicate whether a cell is in drought or not (D_s, drought state). In each cell, if the DI value is below a set threshold (T) and is assigned the value of one, otherwise zero (Eq. 4.4).

$$D_s(t) = \begin{cases} 1 & \text{if } DI(t) \leq T \\ 0 & \text{if } DI(t) > T \end{cases}. \tag{4.4}$$

After, DI is converted into a binary representation of the spatial coverage of droughts. For a region, the PDA is calculated with the area of cells in drought and the region area (Eq. 4.5). This will allow us to represent the spatial variations in a time series spectrum. This process is implemented in the toolbox. It has been considered that extensions to the method will be implemented to create a nonbinary representation that could integrate in a better way droughts and provide more insight into the relative differences of the index values among cells:

$$PDA(t) = 100 \Big/ A_{tot} \cdot \sum_{c=1}^{N} (D_s(t) \cdot A) \tag{4.5}$$

where A is the area of the cell c and A_{tot} is the region area. In this methodology, the magnitude of drought is the PDA value. PDA time series allows the identification of large droughts over a region. Small areas are neglected by applying a second threshold.

2.4   Drought Duration, Severity, and Intensity Computing (Step 3)

This methodology follows Mckee et al. (1993), although hereafter it is extended to be used with the PDA concept used in NCDA. Computing of drought duration (DD) starts at the time step when the PDA lies below the defined threshold. In a PDA series, this threshold is estimated by using the 90th percentile of the low PDA. Therefore the spatiotemporal event starts when the PDA is below the set threshold (T_{PDA}) and ends when it is above the set threshold (Eq. 4.6):

$$DD_j = t_E - t_S \tag{4.6}$$

where j is the jth spatiotemporal event and DD, t_S, and t_E are the drought duration, the start and end time of the event j.

The region under the PDA curve is drought severity (S, expressed as a percentage). This value is a measure of the drought magnitude. S is calculated for each event j with Eq. (4.7):

$$S_j = \sum_{t=t_S}^{t_E} PDA(t).$$

(4.7)

The intensity (I) is calculated as the ratio between S and DD (Eq. 4.8):

$$I_j = S_j/DD_j.$$

(4.8)

This I_j ratio can be interpreted as the mean value of PDA during the time DD_j. Calculation of DD, S, and I is carried out over the entire time series of the PDA. In this methodology, each triplet DD, S, and I are the characteristics of what here is called a spatiotemporal event. It is important to highlight that if the spatial coverage is not large enough at any given time, there is no drought. This method is an extension of the methodology used in Corzo Perez et al. (2011).

2.5   Visualization and Analysis of Results (Step 4)

The STAND toolbox includes five types of plots designed for the analysis and presentation of outcomes: (1) line plot, (2) scatter plot, (3) area chart, (4) colored array, and (5) image plot. Table 4.1 shows the information that can be displayed in each plot.

2.6   Interpolation of Pointwise Data

For the analysis and modeling of catchments, it is common to have pointwise information of hydrometeorological data. This information has to be interpolated spatially to be used before carrying out the spatiotemporal analysis of drought. The STAND toolbox includes an algorithm based on the inverse distance weighted (IDW), where the missing information is estimated by weighting the neighboring known information. The coefficients of the weighting are inversely proportional to the distances between the point of interest and its closest neighbors.

Table 4.1   Plots for the Visualization of Drought-Related Information in the STAND Toolbox

Plot	Outcome(s)
Line	Drought indicator time series (TA)
Scatter	Duration versus deficit (TA), duration versus severity, duration versus intensity (STA)
Area chart	Time series of percentage of drought area (STA)
Colored array	Time series of percentage of drought area (STA)
Image	Spatial distribution of drought indicator, duration, deficit (TA), and area (STA)

STA, Spatiotemporal analysis; *STAND*, Spatio-Temporal ANalysis of Drought; *TA*, Temporal analysis.

3. Case Study and Data

STAND is applied to two case studies: Mexico and India, two countries prone to drought. For Mexico, Standardized Precipitation Index (SPI) time series calculated by the Servicio Meteorológico Nacional (SMN, National Meteorological Service) were used (Table 4.2). SPI is computed by SMN at 362 stations across the country (Fig. 4.2A). SPI uses only precipitation for its calculation and its methodology is described in Mckee et al. (1993, 1995) and WMO (2012). For India (Fig. 4.2B), grid data from the Standardized Precipitation Evaporation Index (SPEI) Global Drought Monitor were used. The difference between precipitation and evapotranspiration is used to calculate SPEI (Vicente-Serrano et al., 2010). The description of both databases is shown in Table 4.2.

Table 4.2   Summary of Drought Indicator Databases

Database	Repository	Temporal Resolution and Coverage	Spatial Resolution and Coverage	Meteorological Data Source (Input)	Main References of Procedure
SPI	SMN[a]	1—24 months, 1951—2017	362 weather stations, Mexico	SMN weather stations	Mckee et al. (1993) and WMO (2012)
SPEI v2.3	SPEI global[b]	1—48 months, 1901—2013	0.5 degrees, globe	CRU TS 3.23[c] (Harris et al., 2014)	Vicente-Serrano et al. (2010) and Beguería et al. (2014)

[a]SMN-Mexico SPI: Standardized Precipitation Index (SPI) from the Servicio Meteorológico Nacional (SMN, National Meteorological Service)-Mexico (http://smn.cna.gob.mx/es/climatologia/monitor-de-sequia/spi).
[b]SPEI global: Standardized Precipitation Evaporation Index (SPEI) Global Drought Monitor (https://digital.csic.es/handle/10261/128892).
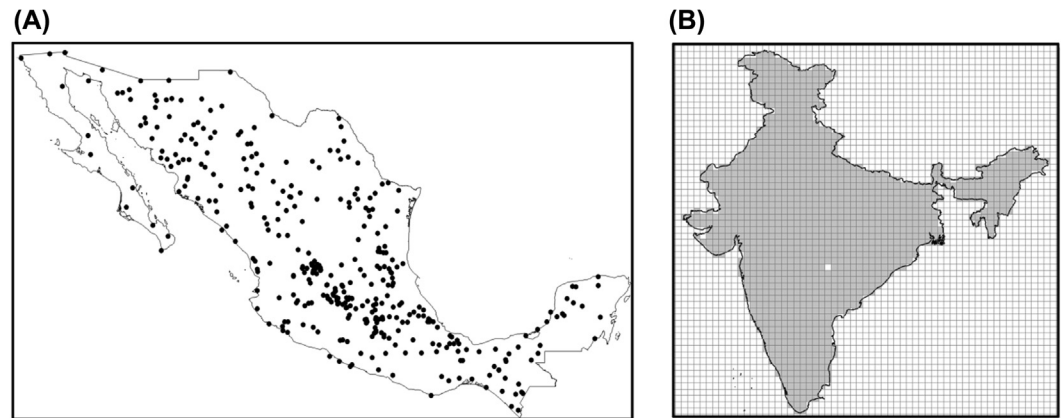[c]Climatic Research Unit time series 3.23.

FIGURE 4.2 (A) 362 weather stations where Standardized Precipitation Index (SPI) is calculated by Servicio Meteorológico Nacional (SMN). (B) Region where 0.5-degree Standardized Precipitation Evaporation Index (SPEI) data were used to analyze drought over India.

4. Experiment Setup

For Mexico and India, the experiments were carried out according to the STAND methodology (Section 2). In both cases, for SPI and SPEI the aggregation period of 6 months was chosen to illustrate the application of STAND. This is indicated with SPI6 and SPEI6, respectively. For the case of Mexico, data were first spatially interpolated to obtain the DI values in a grid with a 0.01 degree resolution. This resolution was considered appropriate to reduce the overlap of points in the same cell.

Temporal analysis was performed to identify regions of critical variations of temporal events through their duration and deficit. Also, the time series of country-average SPI6 and SPEI6 were calculated. Afterward, through NCDA analysis, the drought areas and their percentages (PDAs) were calculated. In both cases, for each cell and each time step, the DI value of -1 was set as the threshold to consider an anomaly as drought or not through ones and zeros, respectively. Following DDRASTIC methodology, durations, severities, and intensities of the spatiotemporal events were calculated (Section 2.4). In the PDA series, the 90th percentile of the low PDA was used as threshold.

Results of the STAND methodology were analyzed through the graphic elements that are included in the toolbox. Results were also compared with local information reported in the Emergency Events Database (EM-DAT, Guha-Sapir, 2018). The most severe drought events were also analyzed.

5. Results and Discussion

5.1 Mexico

5.1.1 Step 1: Temporal Analysis

Fig. 4.3 shows the range of SPI6 values of all the cells for the period $1951-2017$ (67 years). Values from the SPI6 database fluctuate between -6 and 6. Country-average SPI6 is displayed with a colored line. We can identify that in some decades there are country-average SPI6 values lower than threshold -1, for example, the 1970s, 1980s, 1990s, 2000s, and the current decade (2010s). These low peaks indicate months where on average the country presented SPI values lower than -1, which point out large portions of the territory in drought. These results are consistent with that reported in the
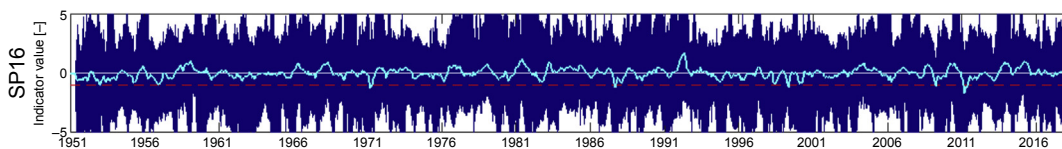

FIGURE 4.3 SPI6 time series per cell. *Colored line* indicates the country-average SPI6 of Mexico.
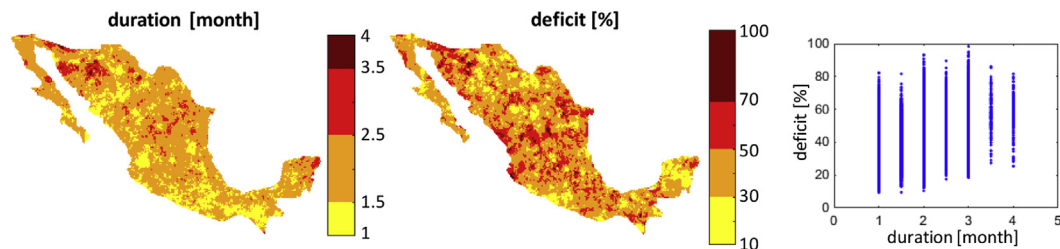
FIGURE 4.4 Median duration and deficit of time series events in Mexico based on SPI6 (1951−2017).

EM-DAT, where, for example, the drought of 2011 is indicated as one of the most impactful in Mexico (Guha-Sapir, 2018).

The spatial distribution of median duration (left) and deficit (center) of the time series events are presented in Fig. 4.4. It is observed that northern Mexico is the zone with the highest density of events with the longest duration and deficit. This was expected since in northern Mexico the arid climate predominates and the monthly precipitation values are the lowest in the country. The maximum of median durations in the region appears to be 4 months, and shorter events are present in central and southern regions. The duration of 1 month seems to be along the whole country showing that these short durations could be noise and should be removed. No linear relationship between median duration and deficit is observed in Fig. 4.4 (right).

5.1.2   Step 2: Spatiotemporal Analysis

Fig. 4.5 presents PDA series calculated for Mexico. It is observed that throughout the decades the spatial extent of droughts fluctuates from zero, reaching in some years peaks even greater than 50%. The PDAs sometimes grow over the months and then decrease, as in 1952−53. On other occasions the PDAs grow suddenly as in 1971 and 2011. In others, the maximum PDAs are between low values as in 1998−2000. The maximum PDA was presented in 2011, possibly indicating that the spatial extent of the drought is an important factor in its impact, since the drought reported in 2011 was one of the worst in Mexico.
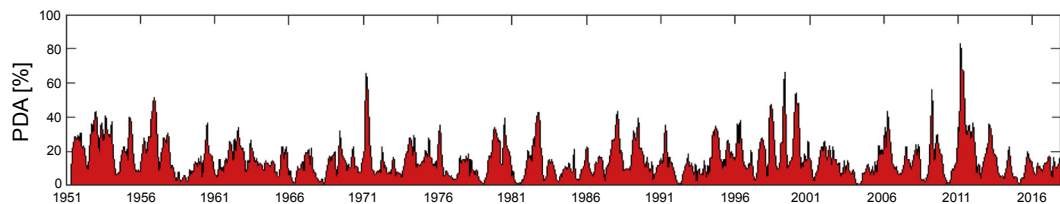

FIGURE 4.5 Area chart with percentages of drought area in Mexico based on SPI6 (1951−2017).
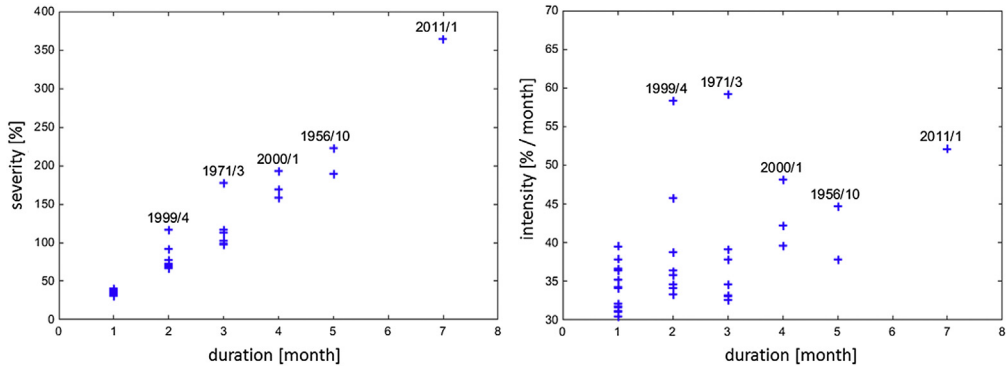
FIGURE 4.6 Duration versus severity (*left*) and duration versus intensity (*right*) of spatiotemporal events in Mexico based on DDRASTIC methodology. Some of the most severe events are indicated.

5.1.3   Step 3: Characterization of Spatiotemporal Events

Duration and severity of spatiotemporal events calculated from PDA series are shown in Fig. 4.6 (left). The year and month of the start of each event are indicated as well in the figure. An almost linear relationship between duration and severity is observed. The event with the longest duration is that of 2011, which started in January and ended in July, lasting 7 months. Four other events with important values of severity are shown: 1956, 1971, 1999, and 2000. Duration versus intensity is presented in Fig. 4.6 (right). It is observed that the event of 1971 presents the maximum intensity. With a duration of 3 months, this event reached an intensity of around 60%/month, i.e., for 3 months the average PDA was 60%. In the event of 2011, average PDA was a little over 50% for 7 months.

5.1.4   Step 4: Visualization

In previous paragraphs, results of the STAND methodology have been presented using graphic elements that are included in the toolbox. In this section, other plots that can be used to display and analyze spatial and spatiotemporal events are shown. PDAs are displayed now in a colored array in Fig. 4.7. Rows make reference to the months of
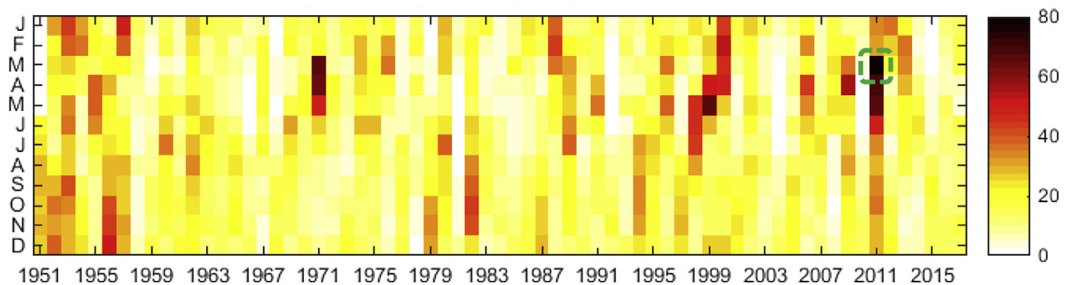

FIGURE 4.7 Percentage of drought area (PDA) for the period 1951–2017 based on SPI6. It is indicated that the highest PDA is in March 2011 (details in Fig. 4.8).
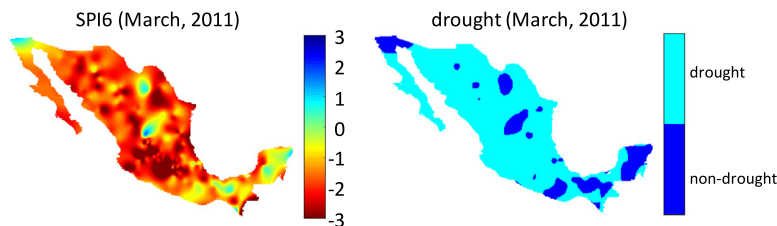
FIGURE 4.8 Spatial distribution of SPI6 and drought area in March 2011.

January to December (J to D) and columns the years from 1951 to 2017. PDAs are displayed on a color scale. Colors white to yellow indicate PDA values of 0%−40%, while orange to dark red indicate PDA values from 40% to 80%. Whitish sections point out periods with small or no PDA values. It is observed that, in general, PDA values greater than 50% occur in the first semester (January to June). The years of 1956, 1957, 1971, 1998, 1999, 2000, 2009, and 2011 present monthly PDAs greater than 50%. The maximum PDA corresponds to March 2011. In this year, values greater than 50% begin in March, continue, and end in June. Fig. 4.8 shows the spatial distribution of SPI6 and the drought area calculated for March 2011. The effect of the interpolation by the IDW method on the spatial distribution of the SPI values is observed. The shape and extent of the drought areas seem to depend on the interpolation method used. Thus it is advisable to perform a sensitivity analysis to study the effect of the chosen interpolation method on the calculation of the PDA.

5.2   India

5.2.1   Step 1: Temporal Analysis

The range of SPEI6 in each cell over India is presented in Fig. 4.9. Also the country-average SPEI6 is displayed (colored line). Values of SPEI6 databases oscillate between −3 and 3. In some decades, country-average SPEI6 values lower than −1 are observed, e.g., the 1900s, 1910s, 2000s, and the current decade. These low peaks point out than in those decades the country had large areas in drought. This is consistent with Bhalme and Mooley (1980) and Guha-Sapir, (2018), where in some of these years, severe droughts were reported.

Fig. 4.10 shows the spatial distribution of median duration (left) and deficit (center) of the time series events in India based on SPEI6 for the period 1901−2013 (113 years).
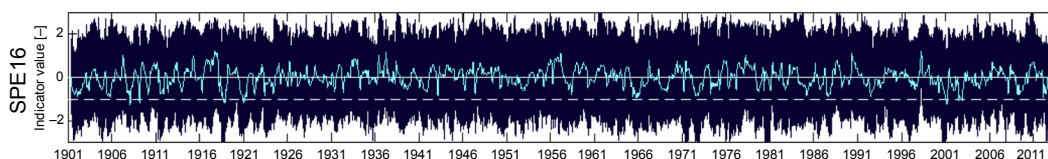

FIGURE 4.9 SPEI6 time series per cell. *Colored line* indicates the country-average SPEI6 of India.
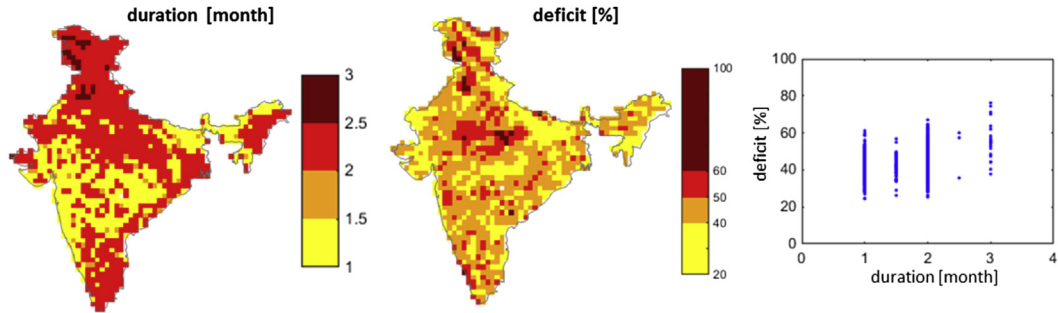
FIGURE 4.10 Median duration and deficit of time series events in India based on SPEI6 (1901−2013).

The longest events are mainly in the north, northeast, and south. On the other hand, deficit is greater in central and north India. The maximum of median durations is observed to be 3 months, and most events have a duration between 2 and 2.5 months. The relationship between median duration and the deficit shown in Fig. 4.10 (right) is not linear, but it is observed that there is a slight positive tendency in the deficit increase as the duration grows.

5.2.2 Step 2: Spatiotemporal Analysis
The time series of PDA calculated for India is shown in Fig. 4.11. The presence of peaks greater than 40% is observed throughout the series. The event of 2001 is the maximum reaching a value of 72%. Other important events are those of 1920, 1972, and 2002. In some of these years, the most severe droughts occurred in India according to Bhalme and Mooley (1980) and Guha-Sapir (2018).

5.2.3 Step 3: Characterization of Spatiotemporal Events
Fig. 4.12 (left) presents duration versus severity of spatiotemporal events calculated from PDAs. The year and month of the start of each event are also indicated in the figure. The relationship between duration and severity seems to be linear. In 1972 the longest event was presented with 9 months of duration, starting in April and ending in December. On the other hand, the event with the maximum severity is that of 1920, which began in October and ended in May 1921, lasting 8 months. Duration versus intensity is presented
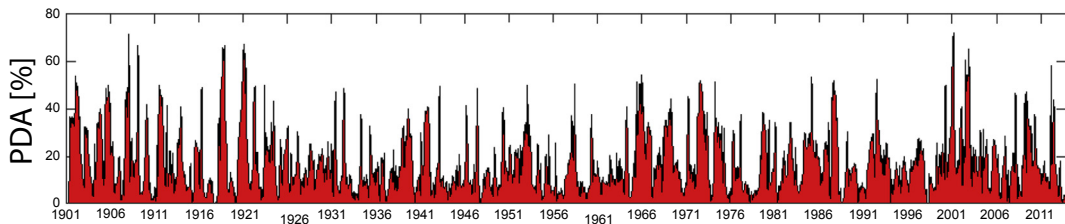

FIGURE 4.11 Area chart with percentages of drought area in India based on SPEI6 (1901−2013).
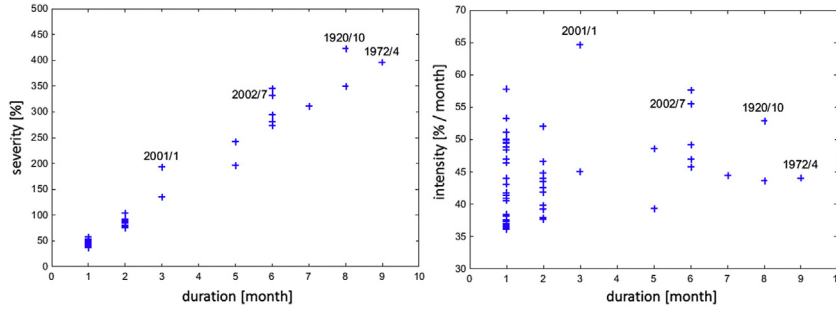
FIGURE 4.12 Duration versus severity (*left*) and duration versus intensity (*right*) of spatiotemporal events in India based on DDRASTIC methodology. Some of the most severe events are indicated.

in Fig. 4.12 (right). It is observed that the event of 2001 is the one of greater intensity with a value of around 65%/month. An important event is that of 1920, which for 8 months averages a value of just over 50% of PDA.

5.2.4   Step 4: Visualization
Outcomes of the STAND methodology were displayed in the previous sections. In this section, other plots to observe and analyze spatial and spatiotemporal events are also shown. In Fig. 4.13 the PDAs are displayed for the period 1901−2013 (113 years). The color scale indicates the percentages. The whitish and yellow spaces indicate periods with null and low values of drought, respectively. Colors orange to dark red refer to values of 50%−100%. Different patterns are observed in the PDA array of Fig. 4.13. For example, a series of successive PDAs greater than 50% that begin in July and last until December are identified, such as the years 1918, 1972, and 2002, to name a few. In some years, the succession of PDAs continues until the following year, for example, 2001−02.

Fig. 4.14 shows how drought areas change in space and time for the years 1920, 1921, 1972, 1973, and 2000−03. This is done to analyze the events of 1920, 1972, 2001, and 2002 presented in the previous section. In the case of India, the PDA threshold is around 36% for the DDRASTIC methodology. Based on this methodology, the 1920 event began in
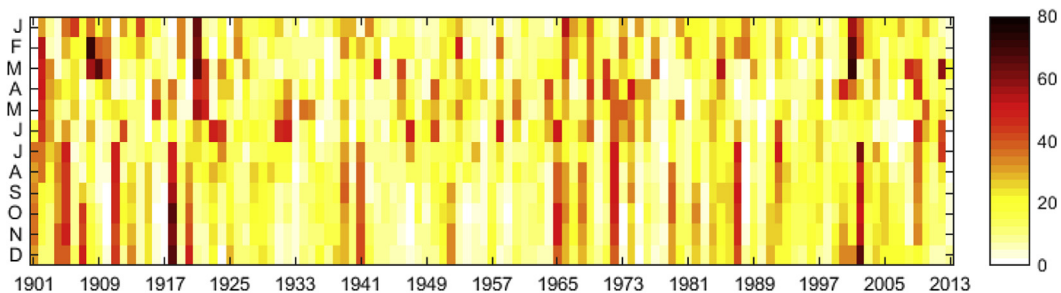

FIGURE 4.13 Percentage of drought area for the period 1901−2013 based on SPEI6.
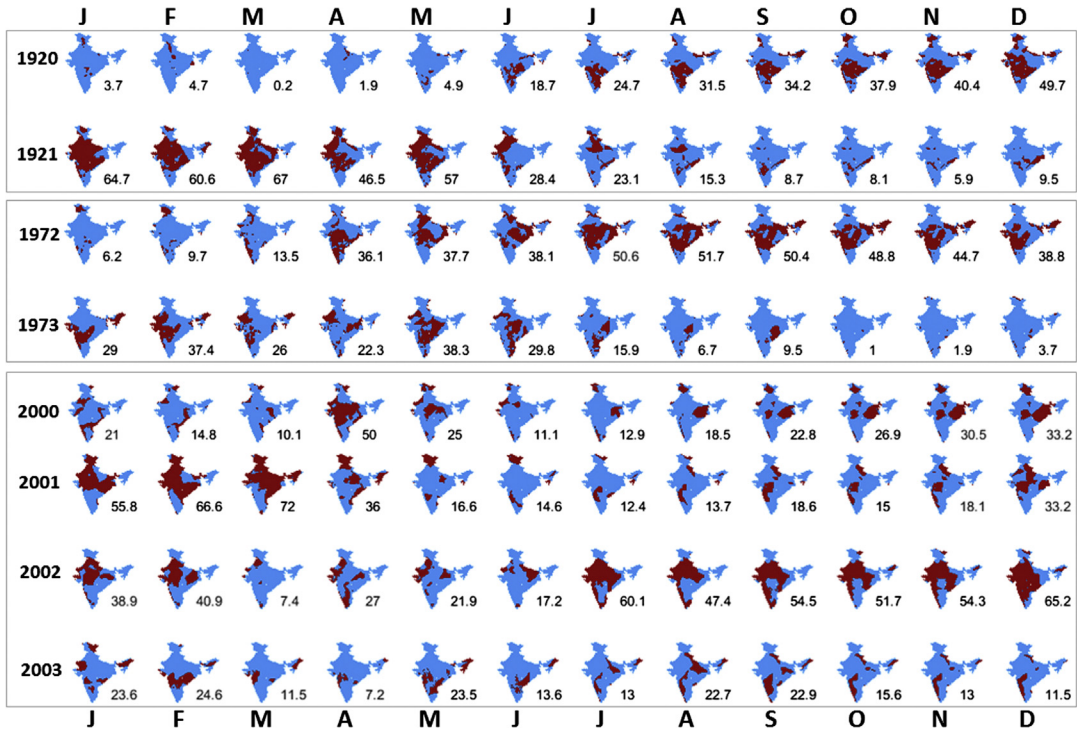
FIGURE 4.14 Spatiotemporal variability of drought areas in India of selected years based on SPEI6. The percentage of drought area is indicated.

October and ended in May 1921, lasting 8 months. For this period, two drought areas are observed mainly in Fig. 4.14, which merged in January 1921. With respect to 1972, the event started in April and ended in December of the same year (9 months). In this case, one area is observed mainly in the central part. The events of 2001 and 2000 seem to be composed of a single drought area as well. The year 2001 began in January and ended in March (3 months), while 2002 began in July and ended in December (6 months). The maximum value of PDA was presented in March 2001 with 72%.

6. Conclusions

The STAND toolbox was introduced and its use was illustrated through two case studies. Two methodologies for the characterization of drought were included within STAND: (1) NCDA analysis and (2) DDRASTIC. It is concluded that the STAND toolbox assisted in the realization of spatiotemporal analysis of drought due to its modules to prepare, process, and visualize drought-related information.

In the case studies for Mexico and India, some findings can be pointed out based on the application of STAND methodology.

6.1   Mexico

- In the decades of the 1970s, 1980s, 1990s, 2000s, and 2010s, the country-average SPI6 values are the lowest. The 2010s seems to be one of the most extreme.
- From the spatial distribution of median duration and deficit of the time series events, it is observed that northern Mexico is the zone with the highest density of events with the longest duration and deficit. The maximum of median durations appears to be 4 months. The shorter events are present in central and southern Mexico.
- The years 1956, 1957, 1971, 1998, 1999, 2000, 2009, and 2011 present monthly PDAs greater than 50%. The maximum PDA was identified in 2011, possibly indicating that the spatial extent of the drought is an important factor in its impact, since the drought reported in 2011 was one of the most severe in Mexico. The effect of the interpolation by the IDW method on the spatial distribution of the SPI values is observed. The shape and extent of the drought areas seem to depend on the interpolation method used. Thus it is advisable to perform a sensitivity analysis to study the effect of the chosen interpolation method on the calculation of PDA.
- The duration and severity of the spatiotemporal events were calculated by the application of DDRASTIC methodology. The event with the longest duration was identified in 2011, which started in January and ended in July, lasting 7 months, according to results based on SPI6. Four other events with important values of severity are 1956, 1971, 1999, and 2000. A linear relationship between duration and severity is observed. On the other hand, the event of 1971 presented the maximum intensity. With a duration of 3 months, this event reached an intensity of around 60%/month, i.e., for 3 months the average PDA was 60%. In the event of 2011, average PDA was a little over 50% for 7 months.

6.2   India

- Decades with the lowest country-average SPEI6 values were the 1900s, 1910s, 2000s, and 2010s. This agrees with what is reported.
- The spatial distribution of median duration and deficit of the time series events show that the longest events are mainly in the north, northeast, and south. On the other hand, deficit is greater in central and north India. The maximum of median durations is observed to be 3 months, and most events have a duration of between 2 and 2.5 months.
- The maximum PDA was found in 2001. It reached a value of 72%. Other important events are 1920, 1972, and 2002. In some of these years, the most severe droughts occurred in India according to the report.
- From the application of DDRASTIC methodology, it is observed that duration and severity of the spatiotemporal events have a linear relationship. In 1972 the longest event was presented with 9 months of duration, starting in April and ending in December. The event with the maximum severity was that of 1920, which began in

October and ended in May 1921, lasting 8 months. On the other hand, the event of 2001 was the one of greater intensity with a value of around 65%/month.

- Analysis of the spatiotemporal events of 1920, 1972, 2001, and 2002, where the most severe are presented according to DDRASTIC methodology, indicates that the event began in October 1920 and ended in May 1921, lasting 8 months. For this period, two drought areas were mainly observed, which merged in January 1921. With respect to 1972, the event started in April and ended in December of the same year (9 months). In this case, one area is observed, mainly in the central part. The events of 2001 and 2000 seem to be composed of a single drought area as well. The year 2001 began in January and ended in March (3 months), while the one in 2002 began in July and ended in December (6 months). The maximum value of PDA was presented in March 2001 with 72%.

The STAND toolbox is available at www.researchgate.net/project/STAND-Spatio-Temporal-ANalysis-of-Drought. A further step in this research is the design and development of charts to show and analyze the variability of the spatiotemporal characteristics of drought. These plots are based on radial diagrams whose methodology and code can be obtained in the same repository shown earlier.

Acknowledgments

References

Bachmair, S., Stahl, K., Collins, K., Hannaford, J., Acreman, M., Svoboda, M., et al., 2016. Drought indicators revisited: the need for a wider consideration of environment and society. Wiley Interdisciplinary Reviews: Water 3 (4), 516−536. https://doi.org/10.1002/wat2.1154.

Beguería, S., Vicente-Serrano, S.M., Reig, F., Latorre, B., 2014. Standardized precipitation evapotranspiration index (SPEI) revisited: parameter fitting, evapotranspiration models, tools, datasets and drought monitoring. International Journal of Climatology 34 (10), 3001−3023. https://doi.org/10.1002/joc.3887.

Below, R., Grover-Kopec, E., Dilley, M., 2007. Documenting drought-related disasters: a global reassessment. The Journal of Environment & Development 16 (3), 328−344. https://doi.org/10.1177/1070496507306222.

Bhalme, H.N., Mooley, D.A., 1980. Large-scale droughts/floods and monsoon circulation. Monthly Weather Review 108 (8), 1197−1211. https://doi.org/10.1175/1520-0493(1980)108<1197:LSDAMC>2.0.CO;2.

Corzo Perez, G.A., Van Huijgevoort, M.H.J., Voß, F., Van Lanen, H.A.J., 2011. On the spatio-temporal analysis of hydrological droughts from global hydrological models. Hydrology and Earth System Sciences 15 (9), 2963−2978. https://doi.org/10.5194/hess-15-2963-2011.

Guha-Sapir, D., January 14, 2018. EM-DAT: The Emergency Events Database. Université catholique de Louvain (UCL) − CRED, Brussels, Belgium. Retrieved from: www.emdat.be.

Hannaford, J., Lloyd-Hughes, B., Keef, C., Parry, S., Prudhomme, C., 2011. Examining the large-scale spatial coherence of European drought using regional indicators of precipitation and streamflow deficit. Hydrological Processes 25 (7), 1146−1162. https://doi.org/10.1002/hyp.7725.

Harris, I., Jones, P.D., Osborn, T.J., Lister, D.H., 2014. Updated high-resolution grids of monthly climatic observations − the CRU TS3.10 dataset. International Journal of Climatology 34 (3), 623−642. https://doi.org/10.1002/joc.3711.

Herrera-Estrada, J.E., Satoh, Y., Sheffield, J., 2017. Spatio-temporal dynamics of global drought. Geophysical Research Letters 2254−2263. https://doi.org/10.1002/2016GL071768.

Hisdal, H., Tallaksen, L.M., 2003. Estimation of regional meteorological and hydrological drought characteristics: a case study for Denmark. Journal of Hydrology 281 (3), 230−247. https://doi.org/10.1016/S0022-1694(03)00233-6.

Lloyd-Hughes, B., 2012. A spatio-temporal structure-based approach to drought characterisation. International Journal of Climatology 32 (3), 406−418. https://doi.org/10.1002/joc.2280.

Mckee, T.B., Doesken, N.J., Kleist, J., January 1993. The relationship of drought frequency and duration to time scales. In: AMS 8th Conference on Applied Climatology, pp. 179−184. Article id: 10490403.

McKee, T.B., Doesken, N.J., Kleist, J., 1995. Drought monitoring with multiple time scales. In: Conference on Applied Climatology.

Mishra, A.K., Singh, V.P., 2010. A review of drought concepts. Journal of Hydrology 391 (1−2), 202−216. https://doi.org/10.1016/j.jhydrol.2010.07.012.

Mishra, A.K., Singh, V.P., 2011. Drought modeling − a review. Journal of Hydrology 403 (1−2), 157−175. https://doi.org/10.1016/j.jhydrol.2011.03.049.

Peters, E., Bier, G., van Lanen, H.A.J., Torfs, P.J.J.F., 2006. Propagation and spatial distribution of drought in a groundwater catchment. Journal of Hydrology 321 (1−4), 257−275. https://doi.org/10.1016/j.jhydrol.2005.08.004.

Sheffield, J., Wood, E.F., 2011. In: Earthscan, P. (Ed.), Drought: Past Problems and Future Scenarios (London).

Sheffield, J., Andreadis, K.M., Wood, E.F., Lettenmaier, D.P., 2009. Global and continental drought in the second half of the twentieth century: severity-area-duration analysis and temporal variability of large-scale events. Journal of Climate 22 (8), 1962−1981. https://doi.org/10.1175/2008JCLI2722.1.

Tallaksen, L.M., Stahl, K., 2014. Spatial and temporal patterns of large-scale droughts in Europe: model dispersion and performance. Geophysical Research Letters 41 (2), 429−434. https://doi.org/10.1002/2013GL058573.

Tallaksen, L.M., Van Lanen, H.A.J., 2004. In: Tallaksen, L.M., Van Lanen, H.A.J. (Eds.), Hydrological Drought − Processes and Estimation Methods for Streamflow and Groundwater, Developments in Water Sciences 48. Elsevier B.V, The Netherlands.

Tallaksen, L.M., Hisdal, H., Van Lanen, H.A.J., 2009. Space-time modelling of catchment scale drought characteristics. Journal of Hydrology 375 (3−4), 363−372. https://doi.org/10.1016/j.jhydrol.2009.06.032.

Van Huijgevoort, M.H.J., Hazenberg, P., van Lanen, H.a.J., Teuling, a.J., Clark, D.B., Folwell, S., Gosling, S.N., Hanasaki, N., Heinke, J., Koirala, S., Stacke, T., Voss, F., Sheffield, J., Uijlenhoet, R., 2013. Global Multimodel Analysis of Drought in Runoff for the Second Half of the Twentieth Century. Journal of Hydrometeorology 14 (5), 1535−1552. https://doi.org/10.1175/JHM-D-12-0186.1.

Van Loon, A.F., 2015. Hydrological drought explained. Wiley Interdisciplinary Reviews: Water 2 (4), 359−392. https://doi.org/10.1002/wat2.1085.

Vicente-Serrano, S.M., Beguería, S., López-Moreno, J.I., 2010. A multiscalar drought index sensitive to global warming: the standardized precipitation evapotranspiration index. Journal of Climate 23 (7), 1696−1718. https://doi.org/10.1175/2009JCLI2909.1.

Vicente-Serrano, S.M., 2006. Differences in spatial patterns of drought on different time scales: an analysis of the Iberian Peninsula. Water Resources Management 20 (1), 37−60. https://doi.org/10.1007/s11269-006-2974-8.

World Meteorological Organisation, 2006. Drought Monitoring and Early Warning: Concepts, Progress and Future Challenges. WMO − No. 1006. Retrieved from: http://www.wamis.org/agm/pubs/brochures/WMO1006e.pdf.

World Meteorological Organisation, 2012. Standardized Precipitation Index User Guide. WMO − No. 1090. Retrieved from: http://www.wamis.org/agm/pubs/SPI/WMO_1090_EN.pdf.

Zaidman, M.D., Rees, H.G., Young, A.R., 2002. Spatio-temporal development of streamflow droughts in north-west Europe. Hydrology and Earth System Sciences 6, 733−751. https://doi.org/10.5194/hess-6-733-2002.